Dominant Mutations in KBTBD13, a Member of the BTB/Kelch Family, Cause Nemaline Myopathy with Cores

Nyamkhishig Sambuughin,[1,*] Kyle S. Yau,[2] Montse Olivé,[3] Rachael M. Duff,[2] Munkhuu Bayarsaikhan,[1] Shajia Lu,[4] Laura Gonzalez-Mera,[3] Padma Sivadorai,[5] Kristen J. Nowak,[2] Gianina Ravenscroft,[2] Frank L. Mastaglia,[6] Kathryn N. North,[7] Biljana Ilkovski,[7] Hannie Kremer,[8] Martin Lammens,[8] Baziel G.M. van Engelen,[8] Vicki Fabian,[5] Phillipa Lamont,[9] Mark R. Davis,[5] Nigel G. Laing,[2] and Lev G. Goldfarb[10]

We identified a member of the BTB/Kelch protein family that is mutated in nemaline myopathy type 6 (NEM6), an autosomal-dominant neuromuscular disorder characterized by the presence of nemaline rods and core lesions in the skeletal myofibers. Analysis of affected families allowed narrowing of the candidate region on chromosome 15q22.31, and mutation screening led to the identification of a previously uncharacterized gene, *KBTBD13*, coding for a hypothetical protein and containing missense mutations that perfectly cosegregate with nemaline myopathy in the studied families. KBTBD13 contains a BTB/POZ domain and five Kelch repeats and is expressed primarily in skeletal and cardiac muscle. The identified disease-associated mutations, C.742C>A (p.Arg248Ser), c.1170G>C (p.Lys390Asn), and c.1222C>T (p.Arg408Cys), located in conserved domains of Kelch repeats, are predicted to disrupt the molecule's beta-propeller blades. Previously identified BTB/POZ/Kelch-domain-containing proteins have been implicated in a broad variety of biological processes, including cytoskeleton modulation, regulation of gene transcription, ubiquitination, and myofibril assembly. The functional role of KBTBD13 in skeletal muscle and the pathogenesis of NEM6 are subjects for further studies.

Nemaline myopathy (NEM) is the most common nondystrophic congenital myopathy that affects mainly infants and children. The presence of thread- or rod-like (nemaline) bodies in affected muscle is the histological hallmark of this myopathy. A variety of distinct clinical types of NEM are recognized and are based on the age at disease onset and the severity of muscle weakness, ranging from a severe, neonatal, and often fatal disease to milder, nonprogressive or slowly progressive disease presenting in infancy, childhood, or adulthood.[1,2] The major symptoms are muscle weakness with hypotrophy of diffuse distribution or limited to the face, neck, and proximal limbs but in some patients extending to respiratory muscles. The pattern of inheritance is also variable; autosomal-recessive and autosomal-dominant forms are known and sporadic cases are reported.[3,4] Mutations causing phenotypically distinct NEM variants have been identified in α-actin (*ACTA1* [MIM 161800]), α-slow tropomyosin and β-tropomyosin (*TPM3* [MIM 609284] and *TPM2* [MIM 60928]), troponin T (*TNNT1* [MIM 605355]), nebulin (*NEB* [MIM 256030]), and cofilin2 (*CFL2* [MIM 610687]). Each known NEM gene encodes components of skeletal muscle sarcomeric thin filaments or regulators of their assembly.[3–5] Despite recent progress, the molecular mechanisms remain unknown in a substantial number of NEM cases.

We previously mapped autosomal-dominant NEM in two pedigrees, Dutch and Australian Dutch, to a locus on chromosome 15q21-q23, with a combined LOD score of 10.65 at marker D15S993.[6] We later identified two additional families, Spanish[7] and Australian-Belgian, featuring a similar phenotype and genetically linked to the same chromosomal locus. This type of nemaline myopathy was named NEM type 6 (NEM6 [MIM 609273]). The clinical phenotype of the 42 studied patients includes poor exercise tolerance, characteristic slowness of movements, gait abnormality, and the development of slowly progressive muscle weakness of the neck and proximal limb muscles beginning in childhood (Table 1). The slowness of movements observed in NEM6 patients is not a characteristic feature in other congenital myopathies.[7,8] The NEM6 patients were unable to run and to correct themselves from falling over. This slowness was constant and was not influenced by the environment. The slowness in NEM6 was correlated to a slower torque generation and a lower rate of relaxation.[7] Muscle biopsies demonstrate strikingly similar cross-family images. These include numerous nemaline rods that form confluent inclusions (Figure 1A) near the Z-disks associated with sarcomere disorganization, but some rods are not colocalized with the Z-disks (Figure 1B). Unstructured cores devoid of

[1]Department of Anesthesiology, Uniformed Services University, Bethesda, MD 20814, USA; [2]Centre for Medical Research, University of Western Australia, Western Australian Institute for Medical Research, QEII Medical Centre, Western Australia 6009, Australia; [3]Institut de Neuropatologia, Department of Pathology and Neuromuscular Unit, Department of Neurology, IDIBELL-Hospital de Bellvitge and CIBERNED, Feixa Llarga s/n, Hospitalet de Llobregat, Barcelona 08907, Spain; [4]National Institute of Arthritis, Musculoskeletal and Skin Diseases, National Institutes of Health, Bethesda, MD 20892, USA; [5]Department of Anatomical Pathology, Royal Perth Hospital, Perth, Western Australia 6000, Australia; [6]Centre for Neuromuscular and Neurological Disorders, University of Western Australia 6009, Australia; [7]Institute for Neuroscience and Muscle Research, The Children's Hospital at Westmead, Westmead 2145, Australia; [8]Department of Neurology, Radboud University Nijmegen Medical Centre, Nijmegen 6500,The Netherlands; [9]Division of Neurosciences, Royal Perth Hospital, Perth, Western Australia 6000, Australia; [10]National Institute of Neurological Disorders and Stroke, National Institutes of Health, Bethesda, MD 20892, USA
*Correspondence: nsambuughin@usuhs.mil
DOI 10.1016/j.ajhg.2010.10.020.

Table 1. Clinical Manifestations in NEM6 Patients

Family	Australian Dutch	Dutch	Spanish	Australian Belgian
Number of studied patients	10	24	4	4
Age at onset	childhood	childhood	childhood	childhood
First symptom	unable to run or jump; difficulties on stairs	unable to run or jump; difficulties on stairs	unable to run or jump; difficulties on stairs	unable to skip or jump
Progression	slow	slow, disabling after age 50 yrs	slow, disabling after age 30 yrs	variable, Gower's maneuver as early as 19 years
Distribution of muscle weakness	neck, proximal, distal in one patient	neck and proximal	proximal and distal; neck in two patients	proximal greater than distal; neck weakness in some
Respiratory insufficiency	no	no	no	no
Muscle atrophy	none	diffuse in the most severely affected patient	deltoids, forearms	none
Other symptoms	movement slowness in one patient	movement slowness	movement slowness	movement slowness in one patient
EMG profile	myogenic	myogenic	myogenic	myogenic
Creatine kinase level	normal	normal	normal	normal
Cardiac abnormalities	none identified	none identified	none identified	none identified

oxidative enzyme activity represent an associated feature of the NEM6 subtype (Figure 1C). A combination of nemaline rods and core lesions has also been seen in some patients with mutations in ryanodine receptor (*RYR1* [MIM 180901]).[9,10] However, it is noteworthy that the core lesions observed in NEM6 differ from the classical sharply demarcated cores observed in central core or core-rod disease associated with mutations in *RYR1*.[7] Another unifying feature of the NEM6 subtype is the predominance and hypertrophy of type 1 (slowly twitching) fibers versus atrophic type 2 (fast) fibers (Figure 1D). This pattern is characteristic of the NEM6 subtype and is

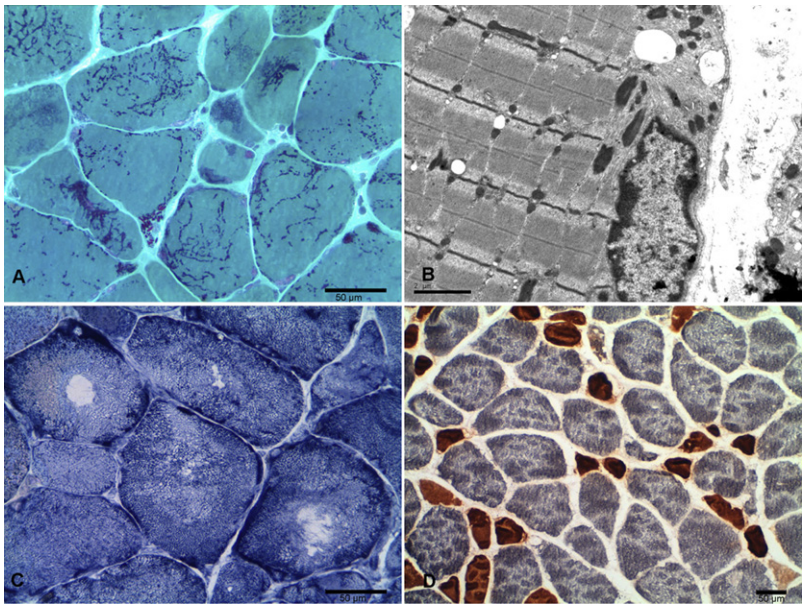

Figure 1. Histochemical, Ultrastructural, and Immunohistochemical Findings in a Muscle Biopsy Sample from the Right Biceps Brachii Muscle Biopsy of the Spanish Family Index Patient

(A) Clusters of nemaline rods on modified trichrome staining forming confluent inclusion in some areas under the sarcolemma and centrally within the cytoplasm (scale bar represents 50 μm).

(B) Electron micrograph showing multiple nemaline rods located under the sarcolemma and near Z-disks (scale bar represents 2 μm). Muscle sample fixed in 2% glutaraldehyde, postfixed with 1% osmium tetroxide, was embedded in araldite. Ultrathin sections were stained with uranyl acetate and lead citrate and were viewed and photographed with a JEOL 1011electron microscope.

(C) Cores devoid of oxidative enzyme activity appear on NADH reaction (scale bar represents 50 μm).

(D) Double-labeling immunohistochemistry for slow (pale) and fast (dark) myosin demonstrating type 1 fiber predominance and hypertrophy versus type 2 fiber atrophy (scale bar represents 50 μm).

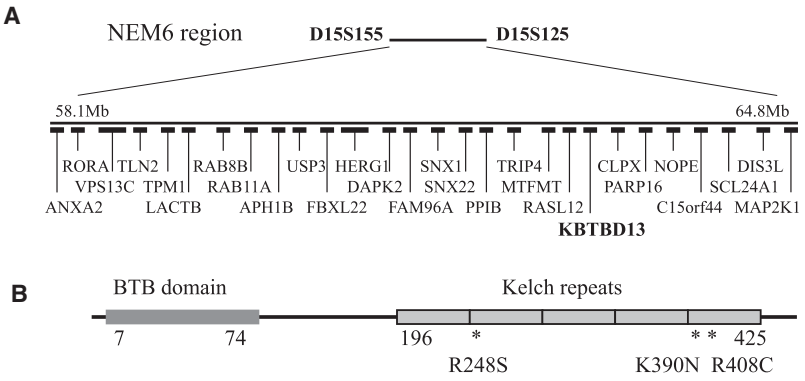

Figure 2. *KBTBD13* Mutations in NEM6 Families
(A) The NEM6 locus is a 6.7 Mb interval delimited by markers D15S155 and D15S125, which physically map between the 58.1 Mb and 68.4 Mb chromosomal positions. The region contains 28 genes expressed in striated muscle.
(B) *KBTBD13* mutations identified in NEM6 patients are located within the highly conserved second and fifth Kelch repeats.
(C) Evolutionary conservation of KBTBD13 domains. The mutated residues are shown in bold.

rarely seen in other subtypes. Rods and cores were jointly present in biopsy samples representing each studied family, affecting 10% to 95% of fibers when measured, and type I fiber predominance and hypertrophy were seen in each case but one (Table S1 available online).

Genetic studies were approved by the institutional review boards of all collaborating institutions and were performed in accordance with the Declaration of Helsinki, and all subjects gave written informed consent prior to participation. We reanalyzed the NEM6 candidate region on the basis of haplotype analysis in three pedigrees and determined that the associated gene is located in a 6.7 Mb region flanked by markers D15S155 and D15S125 on chromosome 15q22.31 (Figure 2A). The region contains more than 70 annotated protein-coding genes (NCBI build 37.1). The most attractive candidate within the NEM6 interval was α-fast tropomyosin (*TPM1* [MIM 191010]), which encodes a thin filament protein expressed in type 2 (fast) skeletal muscle fibers and cardiomyocytes. *TPM1* mutations are known to cause familial hypertrophic cardiomyopathy type 3[11] and dilated cardiomyopathy,[12] and mutations in other tropomyosins cause nemaline myopathy.[13] However, extensive analysis of the coding exons of *TPM1* and its regulatory regions failed to identify mutations in the Dutch, Australian Dutch, or Spanish patients. To rule out the possibility of genomic rearrangements within the candidate region, we surveyed the genome of three affected individuals, using Affimetrix 6.0 SNP chips according to the manufacturer's guidelines. This array contains probes specific for the detection of both SNPs and copy-number variants (CNVs). CNVs were determined with the Partek Genomics Suite (version 6.4, build 6.09.0310) and analyzed with the copy number analysis workflow. An 11.1 kb intragenic deletion in a patient from the Australian Dutch family was identified within the candidate region (data not shown), but this deletion was absent in the patient's affected mother and the index case of the Spanish family, thus excluding disease-specific CNVs.

We then performed mutation screening of 28 genes within the region (Figure 2A). The genes were selected on the basis of the function of encoded proteins and expression in striated muscles. The exons with intronic flanking regions or the cDNA were analyzed for sequence variants in two patients from the Australian Dutch and Spanish families and in two controls. Sequence analysis of candidate genes resulted in the identification of a number of synonymous and nonsynonymous SNPs (Table S2). The nonsynonymous SNPs were then tested in other patients from the same and additional NEM6 families. Potentially disease-causing c.1170G>C (p.Lys390Asn) and c.1222C>T (p.Arg408Cys) mutations were found in a nonannotated and uncharacterized LOC390594 gene that was subsequently designated as "Kelch-repeat and BTB (POZ) domain containing 13" (*KBTBD13* [accession no. NM_001101362.2]) (Figure 2B). The c.1170G>C (p.Lys390Asn) mutation was identified in each patient of the Spanish family, and the c.1222C>T (p.Arg408Cys) mutation perfectly segregated with the disease in the original Dutch, Australian Dutch, and Australian Belgian pedigrees (Figure S1). Analysis of haplotypes based on seven microsatellite markers covering a 1.7 Mb region around *KBTBD13* showed allele sharing between the latter three families (Figure S2), suggesting that a founder effect for the c.1222C>T mutation may exist in the Low Countries of The Netherlands and Belgium. *KBTBD13* was subsequently screened in 14 probands with pathologically diagnosed rod-core disease. A c.742C>A (p.Arg248Ser) variant was found in a single isolated case from Victoria, Australia (Figure 2B). All three *KBTBD13* mutations occurred at amino acid positions conserved through evolution and alter positively charged amino acids (Figure 2C). None of the *KBTBD13* mutations was found in control individuals. The c.1170G>C (p.Lys390Asn) and c.1222C>T (p.Arg408Cys) mutations were absent in 80 Spanish, 52 Dutch, and 84 healthy Americans of European descent. Although the parents

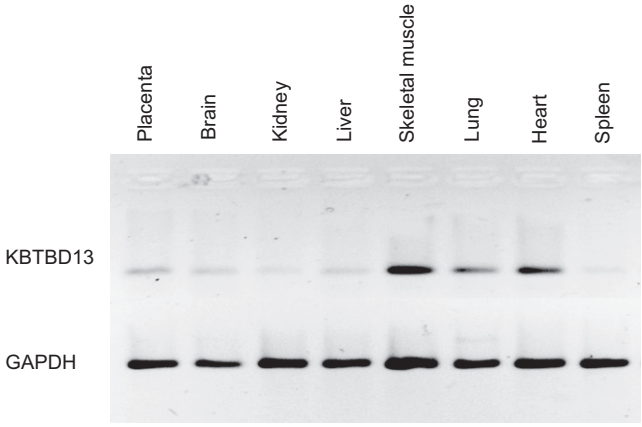

Figure 3. Tissue-Specific Expression of the Mouse KBTBD13
Tissue source is indicated on top of loaded RT-PCR products. GAPDH was used as internal control for normalization of cDNA quantity. The sizes of cDNA fragments are 249 bp for KBTBD13 and 101 bp for GAPDH.

and siblings of the patient with the p.Arg248Ser substitution were not available for further study, we consider this variant as a candidate mutation because it was absent among 148 Australian and 52 Dutch controls.

KBTBD13 is located between nucleotides 65369154 and 65370530 in the NM_001101362.2 sequence of chromosome 15q22.31. The first in-frame ATG of *KBTBD13* is flanked by a Kozak sequence, and the gene has a single exon. The predicted open reading frame comprises 1374 nucleotides encoding a protein, KBTBD13, of 458 amino acids with a molecular mass of 49 kDa (NP_001094832). Highly conserved proteins of a similar size are predicted in vertebrates that share from 51% to 99% identity with human KBTBD13 (data not shown). A single transcript of 3.5 kb was detected in an RNA blot of human skeletal muscle poly A^+ RNA (Figure S3), and a mouse KBTBD13 ortholog (NM_028974; NP_083250) was identified in skeletal and cardiac muscles and lung by RT-PCR testing of multiple tissues (Figure 3). Although KBTBD13 is expressed in the heart, to date no cardiac abnormalities have been identified in affected individuals (Table 1). A focused study of cardiac involvement in NEM6 patients has been performed in two patients of the Spanish family. Electrocardiography, 24 hr Holter monitoring, and echocardiography have not shown any notable alterations.

For determination of subcellular localization, the wild-type human *KBTBD13* cDNA was generated by RT-PCR using skeletal muscle RNA. The c.1222C>T (p.Arg408Cys) mutation was introduced into a wild-type clone through site-directed mutagenesis (Stratagene). The full-length *KBTBD13* transcript was cloned into the pCMV6-AC-MycDDK expression vector (OriGene) and transfected into differentiating C2C12 myotubes and embryonic mouse cardiomyocytes prepared from CD-1 mouse embryos as described previously.[14] Both wild-type and mutant KBTBD13 showed a punctate distribution throughout the cytoplasm in both types of cells. In the cardiomyocytes (Figure 4), KBTBD13 does not colocalize with α-actinin, the major protein component of the Z-disks and the nemaline bodies. This may indicate that the disease mechanisms in NEM6 are fundamentally different from other NEMs. Expression of mutant KBTBD13 showed no gross difference compared to the wild-type KBTBD13 (Figure 4). It is perhaps not surprising, given that NEM6 is a mild, very slowly progressive disorder. However, these experiments are limited to subcellular localization of the protein and do not reveal the pathogenic consequences of mutations. Antibody staining of the endogenous protein is a better tool for the analysis of localization and mutation-specific changes in human NEM6 biopsies and cell models, but no antibodies against KBTBD13 are currently available.

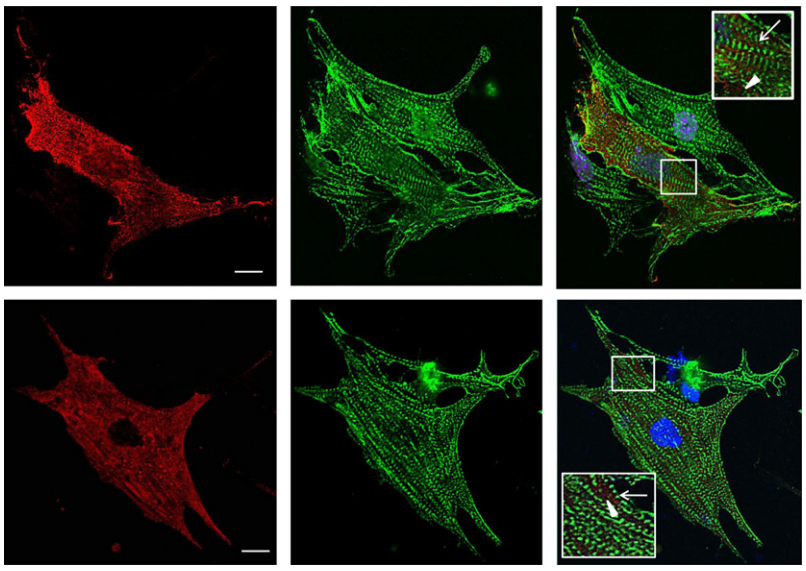

Figure 4. Localization of KBTBD13 Tagged with Myc-Flag in Embryonic Mouse Cardiomyocytes
Top images: wild-type KBTBD13; bottom images: p.Arg408Cys mutant KBTBD13. KBTBD13 is stained in red and α-actinin in green; the nucleus is labeled in blue with DAPI. Inset: higher magnification of boxed areas shows no visible colocalization of the wild-type or mutant KBTBD13 (arrowheads) with α-actinin in striated premyofibrils (arrows). Scale bar represents 10 μm.

KBTBD13 is predicted to contain an N-terminal 68-residue BTB/POZ domain (BTB for Bric-a-brac, Tramtrack, Broad-complex; and POZ for Poxvirus and Zinc-finger), a central α-helical linker region, and a C-terminal Kelch-repeat domain (Figure 2B).[15,16] The Kelch-repeat domain of KBTBD13 consists of five repeats (Figure S4), each containing 42 to 49 amino acids, but the overall homology of the repeats is low. Residues R248, K390, and R408 are located within the highly evolutionarily conserved second and fifth Kelch repeats (Figure 2C and Figure S4), at positions corresponding to $\beta_2$1, $\beta_5$1, and $\beta_5$3 β sheets of the resolved structure of galactose oxidase, a model BTB/Kelch protein,[15] and are predicted to damage the corresponding strands of the molecular β-propeller blades. In light of the pathogenicity of mutations associated with NEM6, KBTBD13 is likely to have a significant though as-yet-unknown role in muscle structure and/or function.

More than 60 proteins of the BTB/Kelch family have been identified,[15–19] of which a few are known to be expressed in skeletal and cardiac muscle: Krp1 or Sarcosin,[18] Muskelin,[19] and KLHL31.[17] BTB/Kelch proteins have been implicated in a broad variety of biological processes, including cytoskeleton modulation, regulation of gene transcription, ubiquitination, cell migration, and myofibril assembly. Although the list of known BTB/Kelch proteins is growing, few have been associated with human disease. Gigaxonin is mutated in patients with giant axonal neuropathy,[20] mutations in KLHL7 cause dominant retinal degeneration,[21] and KLHL9 mutation is associated with distal myopathy.[22] KLHL9 forms a complex with Cullin 3 (Cul-3)-based ubiquitin ligase through its BTB domain, and a KLHL9 alteration diminishes its binding to Cul-3.[22] Similarly, gigaxonin controls the ubiquitin-mediated degradation of cytoskeletal proteins, leading to impaired axonal transport and neuronal death in giant axonal neuropathy.[23] Several other members of the BTB/Kelch family interact with Cul-3 and participate in direct ubiquitination, demonstrating that members of the BTB/Kelch protein families define a new class of substrate-specific adaptors for Cul-3 based ubiquitin ligase.[22–25] Whether this function relates to NEM6 pathogenesis remains to be determined.

In conclusion, we have identified a member of the BTB/Kelch family of proteins that if mutated causes muscle disease characterized by nemaline rod and core formation and muscle weakness, likely through a mechanism different than that of nemaline myopathy associated with mutations in other genes. A combination of gene mapping, positional cloning, mutation screening, and high-throughput copy-number analysis was used to identify the genetic cause of this disease. These findings will promote understanding of the functional role of the growing number of BTB/Kelch proteins, specifically KBTBD13, in skeletal muscle, provide insight into the pathogenesis of NEM6, and stimulate the development of treatments for this childhood-onset disease.

Supplemental Data

Supplemental Data include two tables and four figures and can be found with this article online at http://www.cell.com/AJHG/.

Acknowledgments

The authors would like to thank the members of the affected families for their participation in the study. We thank O. Mungunsukh, USU, for technical advice and for providing RNA from mice tissues. We are grateful to R. Horowits, NIH, for critical comments on the manuscript. The authors thank the Biomedical Instrumentation Center of USU for oligo synthesis, DNA sequencing, and assistance with confocal microscopy. This research was supported by a USU R080CD grant to N.S. M.O. is supported by FIS grant PI08-574 from the Instituto Carlos III, Ministry of Education and Research, Spain. N.G.L. is supported by an Australian National Health and Medical Research Council (NHMRC) fellowship grant, 403904. K.J.N., G.R., and B.I. are supported by NHMRC project grant 403941. This work was supported in part by the Intramural Research Program of the National Institute of Neurological Disorders and Stroke, NIH.

Received: July 19, 2010
Revised: October 9, 2010
Accepted: October 20, 2010
Published online: November 24, 2010

Web Resources

The URLs for data presented herein are as follows:

NCBI Build 37.1, http://www.ncbi.nlm.nih.gov/mapview/
NCBI Nucleotide Database, http://www.ncbi.nlm.nih.gov/nuccore
NCBI Protein Database, http://www.ncbi.nlm.nih.gov/protein
Online Mendelian Inheritance in Man (OMIM), http://www.ncbi.nlm.nih.gov/Omim/

Accession Numbers

The dbSNP accession numbers for the SNPs reported in this paper are ss262957117, ss262957118, and ss262957119. The NCBI accession number for the cDNA sequence reported in this paper is NM_001101362.2.

References

1. North, K.N., Laing, N.G., and Wallgren-Pettersson, C.; The ENMC International Consortium and Nemaline Myopathy. (1997). Nemaline myopathy: current concepts. J. Med. Genet. *34*, 705–713.
2. Ryan, M.M., Schnell, C., Strickland, C.D., Shield, L.K., Morgan, G., Iannaccone, S.T., Laing, N.G., Beggs, A.H., and North, K.N. (2001). Nemaline myopathy: a clinical study of 143 cases. Ann. Neurol. *50*, 312–320.
3. Sanoudou, D., and Beggs, A.H. (2001). Clinical and genetic heterogeneity in nemaline myopathy—a disease of skeletal muscle thin filaments. Trends Mol. Med. *7*, 362–368.
4. Laing, N.G., and Wallgren-Pettersson, C. (2009). 161st ENMC International Workshop on nemaline myopathy and related

disorders, Newcastle upon Tyne, 2008. Neuromuscul Disord. *19*, 300–305.
5. North, K. (2008). What's new in congenital myopathies? Neuromuscul. Disord. *18*, 433–442.
6. Gommans, I.M., Davis, M., Saar, K., Lammens, M., Mastaglia, F., Lamont, P., van Duijnhoven, G., ter Laak, H.J., Reis, A., Vogels, O.J., et al. (2003). A locus on chromosome 15q for a dominantly inherited nemaline myopathy with core-like lesions. Brain *126*, 1545–1551.
7. Olivé, M., Goldfarb, L., Lee, H.S., Zagaa, O., Blokhin, A., Gonzalez-Mera, L., Moreno, D., Laing, N.G., and Sambuughin, N. (2010). Nemaline myopathy type 6: Clinical and myopathological features. Muscle and Nerve, in press.
8. Pauw-Gommans, I.M., Gerrits, K.H., de Haan, A., and van Engelen, B.G. (2006). Muscle slowness in a family with nemaline myopathy. Neuromuscul. Disord. *16*, 477–480.
9. Monnier, N., Romero, N.B., Lerale, J., Nivoche, Y., Qi, D., MacLennan, D.H., Fardeau, M., and Lunardi, J. (2000). An autosomal dominant congenital myopathy with cores and rods is associated with a neomutation in the RYR1 gene encoding the skeletal muscle ryanodine receptor. Hum. Mol. Genet. *9*, 2599–2608.
10. Scacheri, P.C., Hoffman, E.P., Fratkin, J.D., Semino-Mora, C., Senchak, A., Davis, M.R., Laing, N.G., Vedanarayanan, V., and Subramony, S.H. (2000). A novel ryanodine receptor gene mutation causing both cores and rods in congenital myopathy. Neurology *55*, 1689–1696.
11. Thierfelder, L., Watkins, H., MacRae, C., Lamas, R., McKenna, W., Vosberg, H.P., Seidman, J.G., and Seidman, C.E. (1994). Alpha-tropomyosin and cardiac troponin T mutations cause familial hypertrophic cardiomyopathy: a disease of the sarcomere. Cell *77*, 701–712.
12. Olson, T.M., Kishimoto, N.Y., Whitby, F.G., and Michels, V.V. (2001). Mutations that alter the surface charge of alpha-tropomyosin are associated with dilated cardiomyopathy. J. Mol. Cell. Cardiol. *33*, 723–732.
13. Laing, N.G., Wilton, S.D., Akkari, P.A., Dorosz, S., Boundy, K., Kneebone, C., Blumbergs, P., White, S., Watkins, H., Love, D.R., et al. (1995). A mutation in the alpha tropomyosin gene TPM3 associated with autosomal dominant nemaline myopathy. Nat. Genet. *9*, 75–79.
14. Lu, S., Carroll, S.L., Herrera, A.H., Ozanne, B., and Horowits, R. (2003). New N-RAP-binding partners alpha-actinin, filamin and Krp1 detected by yeast two-hybrid screening: implications for myofibril assembly. J. Cell Sci. *116*, 2169–2178.
15. Prag, S., and Adams, J.C. (2003). Molecular phylogeny of the kelch-repeat superfamily reveals an expansion of BTB/kelch proteins in animals. BMC Bioinformatics *4*, 42.
16. Stogios, P.J., Downs, G.S., Jauhal, J.J., Nandra, S.K., and Privé, G.G. (2005). Sequence and structural analysis of BTB domain proteins. Genome Biol. *6*, R82.
17. Abou-Elhamd, A., Cooper, O., and Münsterberg, A. (2009). Klhl31 is associated with skeletal myogenesis and its expression is regulated by myogenic signals and Myf-5. Mech. Dev. *126*, 852–862.
18. Greenberg, C.C., Connelly, P.S., Daniels, M.P., and Horowits, R. (2008). Krp1 (Sarcosin) promotes lateral fusion of myofibril assembly intermediates in cultured mouse cardiomyocytes. Exp. Cell Res. *314*, 1177–1191.
19. Prag, S., De Arcangelis, A., Georges-Labouesse, E., and Adams, J.C. (2007). Regulation of post-translational modifications of muskelin by protein kinase C. Int. J. Biochem. Cell Biol. *39*, 366–378.
20. Bomont, P., Cavalier, L., Blondeau, F., Ben Hamida, C., Belal, S., Tazir, M., Demir, E., Topaloglu, H., Korinthenberg, R., Tüysüz, B., et al. (2000). The gene encoding gigaxonin, a new member of the cytoskeletal BTB/kelch repeat family, is mutated in giant axonal neuropathy. Nat. Genet. *26*, 370–374.
21. Friedman, J.S., Ray, J.W., Waseem, N., Johnson, K., Brooks, M.J., Hugosson, T., Breuer, D., Branham, K.E., Krauth, D.S., Bowne, S.J., et al. (2009). Mutations in a BTB-Kelch protein, KLHL7, cause autosomal-dominant retinitis pigmentosa. Am. J. Hum. Genet. *84*, 792–800.
22. Cirak, S., von Deimling, F., Sachdev, S., Errington, W.J., Herrmann, R., Bönnemann, C., Brockmann, K., Hinderlich, S., Lindner, T.H., Steinbrecher, A., et al. (2010). Kelch-like homologue 9 mutation is associated with an early onset autosomal dominant distal myopathy. Brain *133*, 2123–2135.
23. Allen, E., Ding, J., Wang, W., Pramanik, S., Chou, J., Yau, V., and Yang, Y. (2005). Gigaxonin-controlled degradation of MAP1B light chain is critical to neuronal survival. Nature *438*, 224–228.
24. Furukawa, M., He, Y.J., Borchers, C., and Xiong, Y. (2003). Targeting of protein ubiquitination by BTB-Cullin 3-Roc1 ubiquitin ligases. Nat. Cell Biol. *5*, 1001–1007.
25. Pintard, L., Willems, A., and Peter, M. (2004). Cullin-based ubiquitin ligases: Cul3-BTB complexes join the family. EMBO J. *23*, 1681–1687.